

High performance flower shape MnO₂ for asymmetric supercapacitor device in aqueous electrolyte

Izan Izwan Misnon, Baiju Vidyadharan, Radhiyah Abd Aziz, Rajan Jose*

Nanostructured Renewable Energy Material Laboratory, Faculty of Industrial Sciences & Technology
Universiti Malaysia Pahang, Lebuhraya Tun Razak
26300 Gambang, Kuantan, Pahang
*rjose@ump.edu.my / joserajan@gmail.com

Abstract—A flower shaped MnO₂ have been synthesized using simple and low temperature procedure. Subsequently, an asymmetric supercapacitor is fabricated using MnO₂ and activated carbon as positive and negative electrode in aqueous electrolyte. The supercapacitor was measured at open windows 2.0 V showing energy density of 25.79 Wh/kg at power density of 100 W/kg. The supercapacitor stability was tested at 3 A/g and showing specific capacitance retention of 95% after 850 cycles.

Keywords—supercapacitor; manganese oxide; asymmetric

I. INTRODUCTION

Supercapacitor is an energy storage devices that provide advantages compared to conventional capacitor including high specific capacitance (C_s) and energy density(E_D) [1]. The energy stored in supercapacitor are through ions adsorption on the electrode – electrolyte interface (electrical double layer capacitor, EDLC) and fast and reversible redox reaction (pseudocapacitance, PC) mechanism [2]. Asymmetric supercapacitor (ASC) usually fabricated by combining PC material as positive electrode and high surface area activated carbon (AC) as negative electrode; separated by permeable separator in electrolyte environment. This combination is essential to obtained maximum open potential (1.8 – 2.4 V) as metal oxide alone offer limited open potential (0.8 – 1.2 V) due to water decomposition process. In case of AC, even though the open potential may achieved 2.0 V, this type of symmetric configuration resulted in lower C_s .

The researchers focused on metal oxides and composite development to enhance E_D and power density (P_D) as this type of material is having higher theoretical values that exceed 1000 F/g [3]–[8]. Among them, manganese oxide (MnO₂) is considered as a superior candidate in replacing ruthenium oxide hydrate (RuO₂·xH₂O) as working electrode material due to several factors, including low in cost, availability, non-toxic and environmentally friendly [9].

In this article, MnO₂ is prepared through a simple and low temperature condition. The ASC was prepared in coin cell type assembly using aqueous potassium sulfate (K₂SO₄) electrolyte. This is in order to enhance the open potential of the ASC and on the same time enhance the E_D as E_D is directly proportional to square of open potential. The MnO₂//AC ASC shows a promising open potential of 2.0 V and demonstrated

E_D of 25.79 h/kg at P_D 100 W/kg.

II. EXPERIMENTAL

A. Material Synthesis

The synthesis of MnO₂ was carried out using hydrothermal method. In a typical experiment 4.5 mmol of potassium permanganate [KMnO₄, BDH Chemicals] solution was mixed with 1.5 mmol ammonium persulfate (APS) [(NH₄)₂S₂O₈, Aldrich] in a Teflon lined stainless steel reactor. After being stirred for 20 min, the reactor was kept in an oven at 90 °C for 24 h. After cooling down to room temperature, the brownish precipitate product was filtered; wash thoroughly with DI water until the pH~7, dry at 50 °C for 24 h.

B. Material Characterizations

The MnO₂ were characterized by X-ray diffraction (XRD), field emission scanning electron microscope (FESEM), and transmission electron microscopy (TEM). The XRD patterns were acquired on Miniflex II (Rigaku, Japan) X-ray diffractometer employing CuK_α radiation ($\lambda = 1.5406$ Å) and Ni- filter. Surface morphology of the samples were investigated using a JSM-7800F (JEOL, Japan) FESEM. The crystal structural details were obtained using Tecnai 20 (FEI, USA) operating at 200 kV accelerated voltage.

C. Electrode Fabrication and Supercapacitor Assembly

The positive electrode were prepared by mixing active material, MnO₂ (70 wt.%) with carbon (Super P, 15 wt.%) and polyvinylidene fluoride (PVDF) binder (15 wt%) using N-methyl pyrrolidone (NMP) as a solvent. The above mixture was stirred for 24 h and the slurry obtained thereby was coated onto a pre-cleaned nickel foam (pores per inch; 110 ppi) substrate. The coated electrode was annealed at 60 °C oven 24 h and finally pressed at 5 MPa using hydraulic press.

The negative electrode were prepared following the similar procedure with positive electrode by replacing commercial activated carbon (S_{BET} : 1820 m²/g, Zhejiang Forest Energy Technology Co. Ltd, China) as the active material. Supercapacitor was assemble in coin cell type case (CR2032) using fibrous glassy carbon as separator and using 0.5 M K₂SO₄ electrolyte.

This work was supported by Malaysian Technical Universities Network (MTUN) grant (RDU121201) and University Malaysia Pahang Graduate Research Scheme (GRS 130317).

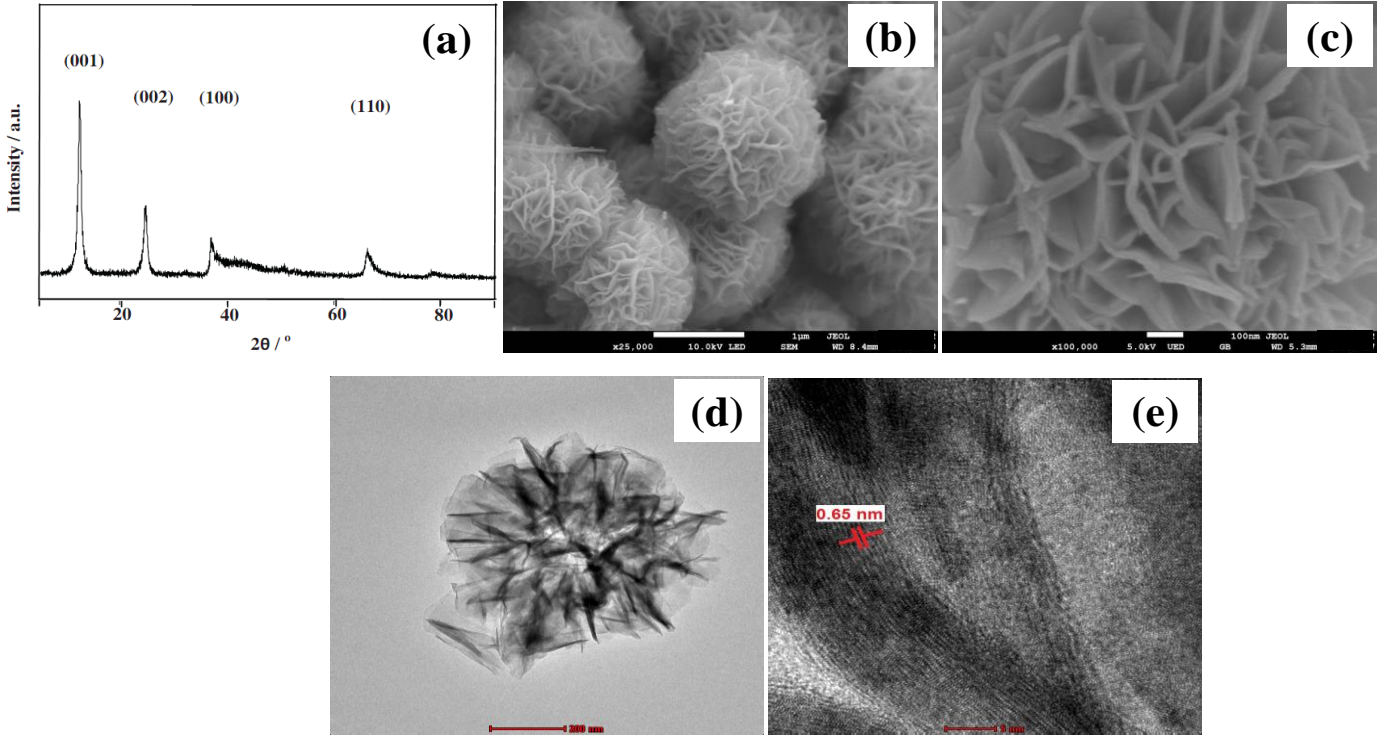


Fig. 1. (a) XRD pattern of MnO₂; FESEM micrograph of flower shaped MnO₂ at (b) low and (c) high magnification; (d) TEM and (e) HRTEM image of MnO₂.

D. Electrochemical Analyses

The electrochemical analysis of cyclic voltammetry (CV), Galvanostatic charge-discharge (CDC) and electrochemical impedance spectroscopy (EIS) were acquired using potentiostat (Autolab PGSTAT 30, Eco Chemie B.V., The Netherlands) employing NOVA 1.9 software. A platinum rod and Ag/AgCl electrode were used as counter and reference electrode for three-electrode configuration analysis. The supercapacitor cycle stability were measured using battery tester (Neware, China).

The specific capacitance (C_S , F/g), energy density (E_D , Wh/kg), power density (P_D , W/kg), internal resistance (I_R , Ω) and coulombic efficiency (η , %) were calculated according to the following Eqs. (1)–(6):

$$C_S (CV) = \frac{1}{m\Delta V} \int_{V_a}^{V_b} i(V) dV \quad (1)$$

$$C_S (CV) = 4 \frac{it}{m\Delta V} \quad (2)$$

$$E_D = \frac{1}{2} C_S (\Delta V)^2 \quad (3)$$

$$P_D = \frac{E_D}{t_d} \quad (4)$$

$$I_R = \frac{V_{IR}}{2i} \quad (5)$$

$$\eta = \frac{t_d}{t_c} \times 100 \quad (6)$$

where m (g) is active mass, v (mV/s) is scan rate, ΔV (V) is the applied potential window (i.e. V_a to V_b), i (A) is current, t_d (s) and t_c (s) are the discharging time and charging time and V_{IR} (V) is the internal resistance potential drop.

III. RESULTS AND DISCUSSION

A. Physicochemical Properties of MnO₂

The XRD pattern of hydrothermal reaction product of MnO₂ is shown in Fig. 1a. The XRD pattern is indexed to the monoclinic potassium birnessite (JCPDF No 43-1456) structure with $C2/m$ space group (No. 12) [10]. The (001) and the (002) planes are typical of the layered structure of δ -MnO₂ whereas the broadened (100) plane indicate crystallized water and formation of water-MnO₂ interlayer [11]. The basal plane spacing calculated from the (001) plane is ~ 0.73 nm, which is the characteristic of the birnessite MnO₂ due to water molecule and intercalated potassium ion.

The FESEM images of MnO₂ at low magnification (Fig. 1b) shows uniform flower-like morphology of MnO₂. Using Image J software measurement, the average diameter of the flowers was ~ 1.23 μ m. A higher magnification FESEM image in Fig. 1c clearly shows that the curly and folded thin nanosheets of thickness ~ 20 nm are branched out from one

central zone.

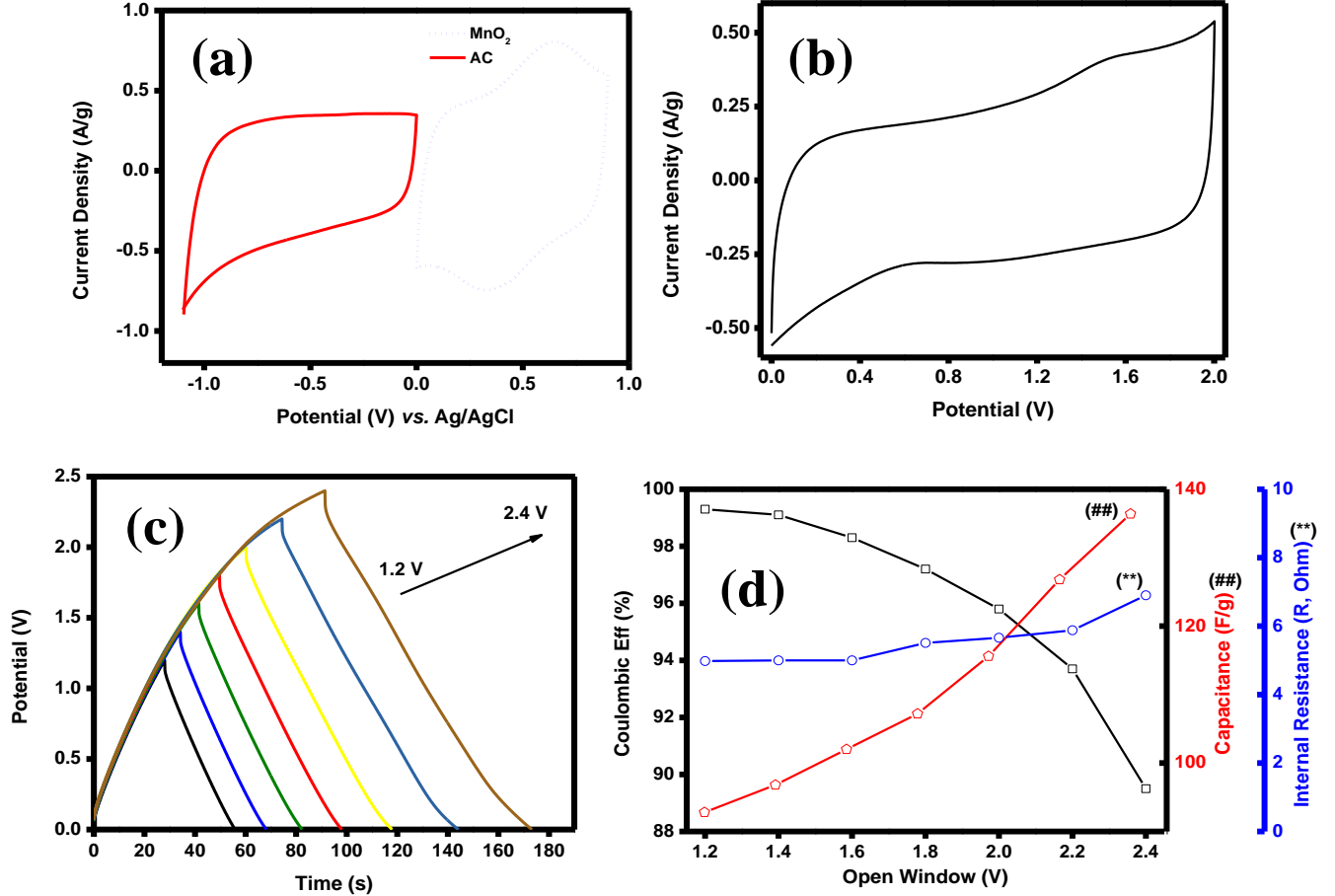


Fig. 2. (a) CV curve for MnO₂ and AC electrode; (b) CV curve for MnO₂//AC supercapacitor at 10 mV/s; (c) CDC curve at current density of 1 A/g for potential range 1.2 – 2.4 V; (d) Variation of η , C_S and I_R for different potential.

The bright field TEM image of the MnO₂ is shown in Fig. 1d. The image indicates that the particles have a coronal spherical morphology, which in turn composed of multilayer hierarchical nanosheets. These curly nanosheets in the sphere are grown from a core during hydrothermal reaction. A high resolution TEM (HRTEM) image of a nanosheet is in Fig. 1e. The measured spacing along the (001) plane is ~ 0.65 nm in HRTEM, which is lower than that observed in the XRD pattern (~ 0.73 nm). This lowering is due to the evaporation of interlayer water molecules under the high energy electron beam irradiation [12].

B. Determination of MnO₂//AC Mass Ratio

To balance the charge (q) and maximize C_S , the mass ratio of positive and negative electrode need to be measured. The individual CV scan of MnO₂ and AC is shown in Fig. 2a. The MnO₂ electrode potential window is in range 0.0 to 0.9 V whereas for AC is in range -1.1 to 0.0 V, in order to archive supercapacitor working potential of 2.0 V. The CV was measured at scan rate 10 mV/s.

The mass ratio of MnO₂ to AC electrode is 0.89, calculated according to Eq. (7).

$$\frac{m_+}{m_-} = \frac{C_{S-} \times \Delta V_-}{C_{S+} \times \Delta V_+} \quad (7)$$

C. Supercapacitor Performance Analysis

The MnO₂//AC asymmetric supercapacitor CV curve at scan rate 10 mV/s is shown in Fig. 2b. It shows that near rectangular CV shape in 2.0 V potential range. The calculated C_S at this scan rate is 54 F/g.

To understand the maximum open potential of MnO₂//AC capability, the CDC at 1 A/g was measure in potential range 1.2 to 2.4 V. The CDC curve for CDC at different potential is shown in Fig. 2c. The curve shows symmetric triangle of charge and discharge; indicate that the optimum reversibility during charging and discharging. The relation of η , C_S and I_R is shown in Fig. 2d. The η is showing decrease trend respect to increased open potential where the efficiency drops from

99.3% at 1.2 V to 89.5% at 2.4 V. The C_S and I_R , however, increase respect to increasing open potential. The C_S is increased from 93 to 137 F/g and the I_R increased from 4.98 to 6.90 Ω . The optimize supercapacitor should having higher η and C_S but minimum I_R . Thus, open potential of 2.0 V is the most promising for MnO_2/AC system.

Then, the performance of MnO_2/AC was tested at different current densities ranging from 3 to 0.1 A/g and the CDC curve is shown in Fig. 3a. Near triangle shape for each CDC test indicate that high reversibility of the supercapacitor for each current density. Clearly, as the current density decrease, the discharge time was also increased. This phenomenon related to the higher fraction of active surfaces are involve in the intercalation – deintercalation of electrolyte ions at lower current density. The ions have slower time to intercate and accumulate on the active site, hence increased the C_S .

The relation of η , C_S and I_R for CDC analysis at different current density was shown in Fig. 3b. Similar to analysis in Fig. 2d, the η is showing decrease trend respect to decrease current densities where the efficiency is 95.2% at 3 A/g, increased to 97.4% (1 A/g) and decrease to 86.1% at 0.1 A/g. The C_S is dramatically increased from 96 F/g at 3 A/g to 186 F/g at 0.1 A/g. The same trend observed to the I_R where constant increase from 3.33 to 5.95 Ω . In this current density range, the E_D are 13.33, 16.39, 18.28, 19.83 and 25.79 Wh/kg at P_D of 3000, 1000, 500, 300 and 100 W/kg for current density of 3, 1, 0.5, 0.3 and 0.1 A/g, respectively. The ragone plot of E_D versus P_D is shown in Fig. 3c.

The MnO_2/AC supercapacitor was tested for cell stability test for 850 cycles and the evidence was shown in Fig. 3d. the device show promising electrochemical stability with the C_S retention ~ 95% after the end of cycle. The η is unchanged at the end of the stability cycle and shows ~94% throughout the test.

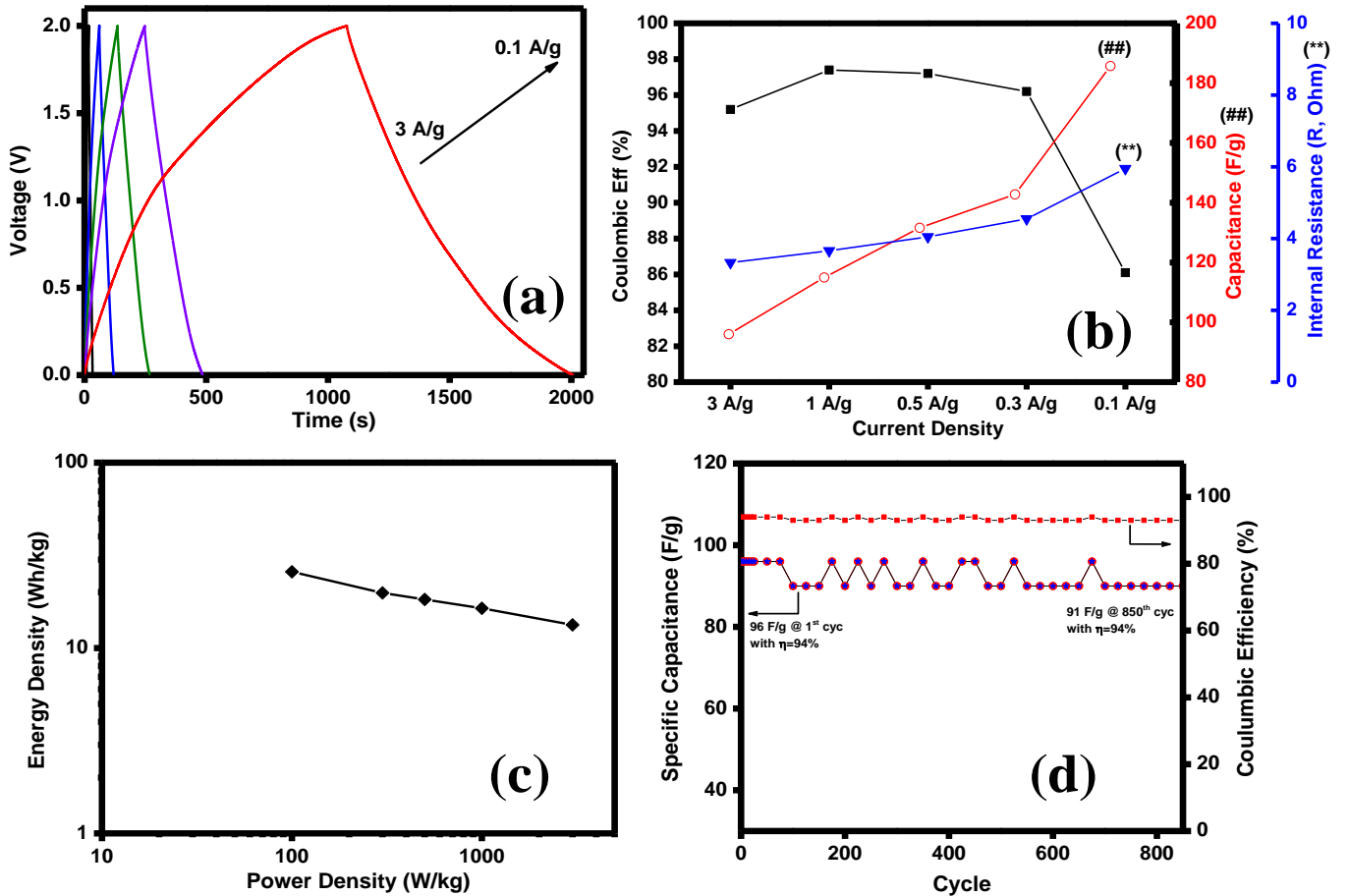
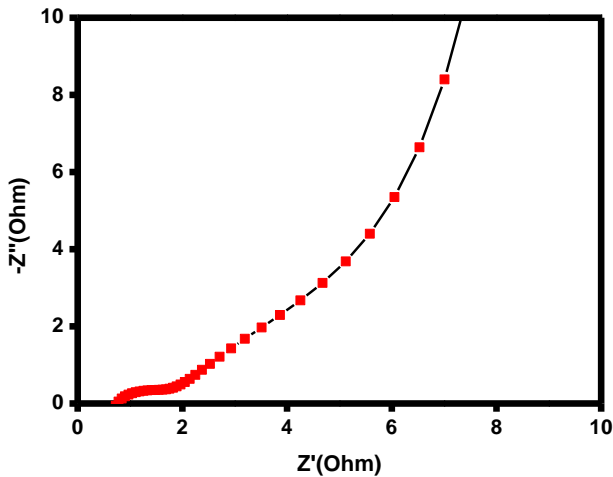


Fig. 3: (a) CDC curve at current densities range from 3 – 0.1 A/g; (b) Variation of η , C_S and I_R for different current densities; (c) Ragone plot of MnO_2/AC supercapacitor; (d) Cycle stability test of MnO_2/AC supercapacitor.

Table 1: Comparison of MnO₂ based ASC device.

Positive electrode	Negative electrode	Electrolyte	Open Potential	C _s (F/g) @ rate behavior	Power (kW/kg)	Energy (Wh/kg)	R _s	Ref.
MnO ₂ (amorphous)	AC	0.1M K ₂ SO ₄	0 – 2.2 V	31 (0.55 A/g)	0.605	17.3		[13]
(Y- α -MnO ₂)	AC	1M LiOH	0.5 – 1.5 V	62.4 (100 mA/g)		19.5	~0.02	[14]
α -MnO ₂	AC	0.1M K ₂ SO ₄	0 – 2.0 V	21 (2.5 mA/cm ²)	-	11.7	1.3	[15]
MnO ₂ nanorod	AC	0.5M K ₂ SO ₄	0 – 1.8 V	53.7 (2C)	2	17	-	[16]
α -MnO ₂	AC	0.5M Na ₂ SO ₄	0 – 1.8 V	23.1 (12.74 mA/cm ²)	14.7(P _{max})	10.4		[17]
MnO ₂ -NF	Graphene Hydrogel	0.5M Na ₂ SO ₄	0 – 2.0 V	41.7 (1 A/g) 26.8 (10 A/g)	1 (1 A/g) 10 (10 A/g)	23.2 (1 A/g) 14.9 (10A/g)	4.9	[18]
δ -MnO ₂	AC	1M Na ₂ SO ₄	0 – 1.6 V	-	0.4 4.0	20.9 8.0	-	[19]
MnO ₂ (amorphous)	AC	2M MgCl ₂ 2M CaCl ₂ 2M KCl	0 – 1.8 V 0 – 2.0 V 0 – 2.0 V	45 (10 mV/s) 40 (10 mV/s) 35 (10 mV/s)	1.0	20 22.5 18	1.08 1.08 0.59	[20]
α -MnO ₂ /CNT	AC	2M KNO ₃	0 – 2.0 V	35 (2 mV/s)	123 (P _{max})	21	0.54	[21]
δ -MnO ₂	AC	0.5 M K ₂ SO ₄	0 – 2.0 V	32.9 F/g (1A/g) 54 F/g (10mV/s)	0.3 24(P _{max})	19.8 25.79	0.76	This work

Table 1 summarize recently published MnO₂ and AC based ASC. The performance shown by this study shows that the device is comparable and most cases is superior with previous report. Finally, the Nyquist plot from EIS measurement of the MnO₂//AC supercapacitor device is shown in Fig. 4. The EIS recorded in the frequency range 10 kHz – 10 mHz at a bias voltage of 0.1 V. The EIS spectrum of supercapacitors is routinely deconvoluted into three sections corresponding to three processes offering (i) series resistance (R_s); (ii) Warburg ion diffusion; and (iii) capacitive behavior.

Fig 4: Nyquist plot of MnO₂//AC supercapacitor device.

The R_s, determined from the high frequency off-set in the real part of complex impedance of the EIS spectrum are

contributed by three main factors viz. (i) electrolyte resistance, (ii) electrode resistance and (iii) electrode – electrolyte resistance. The R_s value for the device is 0.76 Ω . The diameter of semicircle at the high frequency range is due to kinetic resistance to the transfer, known as charge transfer resistance (R_{ct}). The R_{ct} value is 0.79 Ω , result from kinetic transfer of combination of MnO₂ and AC electrode. At the The equivalent distributed resistance (R_d) was obtained from the linear projection of the vertical region of Nyquist plot to the x- intercept on the real impedance and subtracting the R_s from the intersection [22]. The R_d arises from the ions diffusion resistance into the porous (micropores and mesopores) network of MnO₂//AC supercapacitor device. The calculated R_d value for the device is 0.72 Ω .

D. Conclusion

In conclusion, we have synthesis flower shaped MnO₂ and fabricated MnO₂//AC ASC device in aqueous electrolyte. The performance of the device is studied and shows the E_D of 25.79 Wh/kg at P_D 100 W/kg. The stability of the device has been study and shows ~ 95% C_s retention, promising to build energy storage device in the proposed system.

ACKNOWLEDGMENT

The authors thank Zhejiang Forest Energy Technology Co. Ltd for activated carbon sample.

REFERENCES

- [1] B. E. Convey, *Electrochemical Supercapacitors: Scientific Fundamentals and Technological Applications*. New York: Kluwer Academic Press/Plenum Publishers, 1999.
- [2] P. Simon and Y. Gogotsi, "Materials for electrochemical capacitors," *Nat Mater*, vol. 7, no. 11, pp. 845–854, Nov. 2008.
- [3] M. Toupin, T. Brousse, and D. Bélanger, "Influence of Microstructure on the Charge Storage Properties of Chemically Synthesized Manganese Dioxide," *Chem. Mater.*, vol. 14, no. 9, pp. 3946–3952, 2002.
- [4] K. Liang, X. Tang, and W. Hu, "High-performance three-dimensional nanoporous NiO film as a supercapacitor electrode," *Journal of Materials Chemistry*, vol. 22, no. 22, p. 11062, 2012.
- [5] F. Zhang, C. Yuan, X. Lu, L. Zhang, Q. Che, and X. Zhang, "Facile growth of mesoporous Co₃O₄ nanowire arrays on Ni foam for high performance electrochemical capacitors," *Journal of Power Sources*, vol. 203, pp. 250–256, Apr. 2012.
- [6] B. Vidyadharan, R. A. Aziz, I. I. Misnon, G. M. Anil Kumar, J. Ismail, M. M. Yusoff, and R. Jose, "High energy and power density asymmetric supercapacitors using electrospun cobalt oxide nanowire anode," *Journal of Power Sources*, vol. 270, pp. 526–535, Dec. 2014.
- [7] B. Vidyadharan, I. I. Misnon, R. A. Aziz, K. P. Padmasree, M. M. Yusoff, and R. Jose, "Superior supercapacitive performance in electrospun copper oxide nanowire electrodes," *Journal of Materials Chemistry A*, vol. 2, no. 18, p. 6578, 2014.
- [8] B. Vidyadharan, N. K. M. Zain, I. I. Misnon, R. A. Aziz, J. Ismail, M. M. Yusoff, and R. Jose, "High performance supercapacitor electrodes from electrospun nickel oxide nanowires," *Journal of Alloys and Compounds*, vol. 610, pp. 143–150, Oct. 2014.
- [9] I. I. Misnon, R. A. Aziz, N. K. M. Zain, B. Vidyadharan, S. G. Krishnan, and R. Jose, "High performance MnO₂ nanoflower electrode and the relationship between solvated ion size and specific capacitance in highly conductive electrolytes," *Materials Research Bulletin*, vol. 57, pp. 221–230, Sep. 2014.
- [10] O. Ghodbane, J.-L. Pascal, and F. Favier, "Microstructural Effects on Charge-Storage Properties in MnO₂-Based Electrochemical Supercapacitors," *ACS Applied Materials & Interfaces*, vol. 1, no. 5, pp. 1130–1139, May 2009.
- [11] T. T. Truong, Y. Liu, Y. Ren, L. Trahey, and Y. Sun, "Morphological and Crystalline Evolution of Nanostructured MnO₂ and Its Application in Lithium–Air Batteries," *ACS Nano*, vol. 6, no. 9, pp. 8067–8077, Sep. 2012.
- [12] J. Liu, J. Jiang, C. Cheng, H. Li, J. Zhang, H. Gong, and H. J. Fan, "Co₃O₄ Nanowire@MnO₂ Ultrathin Nanosheet Core/Shell Arrays: A New Class of High-Performance Pseudocapacitive Materials," *Advanced Materials*, vol. 23, no. 18, pp. 2076–2081, May 2011.
- [13] T. Cottineau, M. Toupin, T. Delahaye, T. Brousse, and D. Bélanger, "Nanostructured transition metal oxides for aqueous hybrid electrochemical supercapacitors," *Applied Physics A*, vol. 82, no. 4, pp. 599–606, Nov. 2005.
- [14] A. Yuan and Q. Zhang, "A novel hybrid manganese dioxide/activated carbon supercapacitor using lithium hydroxide electrolyte," *Electrochemistry Communications*, vol. 8, no. 7, pp. 1173–1178, Jul. 2006.
- [15] T. Brousse, P.-L. Taberna, O. Crosnier, R. Dugas, P. Guillemet, Y. Scudeller, Y. Zhou, F. Favier, D. Bélanger, and P. Simon, "Long-term cycling behavior of asymmetric activated carbon/MnO₂ aqueous electrochemical supercapacitor," *Journal of Power Sources*, vol. 173, no. 1, pp. 633–641, Nov. 2007.
- [16] Q. Qu, P. Zhang, B. Wang, Y. Chen, S. Tian, Y. Wu, and R. Holze, "Electrochemical Performance of MnO₂ Nanorods in Neutral Aqueous Electrolytes as a Cathode for Asymmetric Supercapacitors," *The Journal of Physical Chemistry C*, vol. 113, no. 31, pp. 14020–14027, Aug. 2009.
- [17] Y.-T. Wang, A.-H. Lu, H.-L. Zhang, and W.-C. Li, "Synthesis of Nanostructured Mesoporous Manganese Oxides with Three-Dimensional Frameworks and Their Application in Supercapacitors," *The Journal of Physical Chemistry C*, vol. 115, no. 13, pp. 5413–5421, Apr. 2011.
- [18] H. Gao, F. Xiao, C. B. Ching, and H. Duan, "High-Performance Asymmetric Supercapacitor Based on Graphene Hydrogel and Nanostructured MnO₂," *ACS Applied Materials & Interfaces*, vol. 4, no. 5, pp. 2801–2810, May 2012.
- [19] G. Zhu, L. Deng, J. Wang, L. Kang, and Z.-H. Liu, "Hydrothermal preparation and the capacitance of hierarchical MnO₂ nanoflower," *Colloids and Surfaces A: Physicochemical and Engineering Aspects*, vol. 434, pp. 42–48, Oct. 2013.
- [20] T. Tomko, R. Rajagopalan, M. Lanagan, and H. C. Foley, "High energy density capacitor using coal tar pitch derived nanoporous carbon/MnO₂ electrodes in aqueous electrolytes," *Journal of Power Sources*, vol. 196, no. 4, pp. 2380–2386, Feb. 2011.
- [21] V. Khomenko, E. Raymundo-Piñero, and F. Béguin, "Optimisation of an asymmetric manganese oxide/activated carbon capacitor working at 2V in aqueous medium," *Journal of Power Sources*, vol. 153, no. 1, pp. 183–190, Jan. 2006.
- [22] R. Kötz and M. Carlen, "Principles and applications of electrochemical capacitors," *Electrochimica Acta*, vol. 45, no. 15–16, pp. 2483–2498, May 2000.